East Asian Journal on Applied Mathematics
doi: 10.4208/eajam.160909.310310a

Vol. **1**, No. 1, pp. 1-19
February 2011

Modified Verlet Method Involving Second-Order Mid-Point Rule Applied to Balls Falling in One-Dimensional Potentials

Hidenori Yasuda*

Department of Mathematics, Faculty of Science, Josai University, 1-1 Keyakidai, Sakado, Saitama, Japan.

Received 16 September 2009; Accepted (in revised version) 31 March 2010

Available online 26 October 2010

Abstract. A modified Verlet method which involves a kind of mid-point rule is constructed and applied to the one-dimensional motion of elastic balls of finite size, falling under constant gravity in space and then under the chemical potential in the interface region of phase separation within a two-liquid film. When applied to the simulation of two balls falling under constant gravity in space, the new method is found to be computationally superior to the usual Verlet method and to Runge–Kutta methods, as it allows a larger time step for comparable accuracy. The main purpose of this paper is to develop an efficient numerical method to simulate balls in the interface region of phase separation within the two-liquid film, where the ball motion is coupled with two-phase flow. The two-phase flow in the film is described via shallow water equations, using an invariant finite difference scheme that accurately resolves the interface region. A larger time step in computing the ball motion, more comparable with the time step in computing the two-phase flow, is a significant advantage. The computational efficiency of the new method in the coupled problem is demonstrated for the case of four elastic balls in the two-liquid film.

AMS subject classifications: 65L12, 65M06, 65P10

Key words: Verlet method, falling balls, first return map, phase separation, shallow water equations.

1. Introduction

The main purpose of this paper is to develop an efficient numerical method to simulate the motion of elastic balls of finite size in immiscible two-liquid films. The phase separates in immiscible films, and the balls are expected to align near the phase separation interface in a kind of self-organisation process related to problems of nanotechnology [8, 18]. Since film phenomena are quite complex, the simulation in this paper is restricted to one

*Corresponding author. *Email address:* yasuda@math.josai.ac.jp (H. Yasuda)

dimension – i.e. the balls (that may collide) fall in a straight line to the bottom of the phase separation potential in the two-phase flow.

Falling ball problems are not easy to analyse. However, balls falling in space under constant gravity have been studied with reference to ergodic theory [4]. In the case of point masses moving in one dimension above a fixed floor, when the upper point masses are lighter than the lower ones it has been proven mathematically that the system has some non-vanishing Lyapunov exponents almost everywhere, and becomes chaotic [16, 17]. For two point masses, there is typical Kolmogorov–Arnold–Moser behaviour when the upper mass is heavier than the lower one, where quasi-periodic and chaotic trajectories coexist in the phase space [15]. Related numerical integration must be performed with high accuracy, and lengthy simulations of falling balls have been undertaken using the symplectic Verlet method.

The main difficulty encountered in previous simulations of the motion of elastic balls of finite size in immiscible two-liquid films was the significantly smaller time step required in the Verlet method than the time step permitted for the flow computation by the CFL (Courant-Friedrichs-Lewy) condition, for a given accuracy. This led the author to construct the modified Verlet method involving the second-order mid-point rule adopted in this paper – i.e. to allow larger time steps for the simulation of the ball motion, more compatible with the time steps allowed in the invariant finite difference scheme used to solve the two-phase shallow-water equations invoked [14].

2. Two Balls Falling Under Constant Gravity and the Modified Verlet Method Involving the Second-Order Mid-Point Rule

In this Section, the modified Verlet method involving the second-order mid-point rule is constructed and applied to the case of two elastic balls of finite size falling vertically under constant gravity above a fixed rigid horizontal floor. This new method is first used in two simpler test problems – viz. the harmonic oscillator and the case of a single bouncing ball. When applied to the two balls falling in space, the new method is then shown to be more efficient than either the usual Verlet or various Runge-Kutta methods.

2.1. Mathematical model

The motion of two balls falling in one dimension under constant gravity above the fixed floor is governed by the system of equations

$$\frac{dz_i}{dt} = v_i \,, \tag{2.1}$$

$$\frac{dv_i}{dt} = f_i\left(z_1, z_2\right) \,, \quad i = 1, 2. \tag{2.2}$$

Here z denotes the vertical position of a ball above the horizontal floor, v the corresponding vertical velocity of the ball, t the time, f represents the acceleration, and the subscripts 1

and 2 denote the lower and upper ball, respectively. The vertical acceleration consists of a gravity term and an impact stress term – i.e.

$$f_1\left(z_1,z_2\right) = -g + f_{1s}\left(z_1\right)/m_1 - f_{12}\left(\mathrm{z}_1,z_2\right)/m_1, \tag{2.3}$$
$$f_2\left(z_1,z_2\right) = -g + f_{12}\left(\mathrm{z}_1,z_2\right)/m_2, \tag{2.4}$$

where g denotes the gravitational acceleration, m_i the respective ball mass ($i = 1,2$), f_{1s} the force attributable to the impact stress between the lower ball and the floor, and f_{12} the force of impact between the two balls.

Since it is assumed the balls are elastic, suitable impact stresses calculated using Hertz theory [11] are

$$f_{1s} = k\cdot\left(x_1\right)^{\frac{3}{2}}, \quad x_1 = \max\left(R - z_1, 0\right), \tag{2.5}$$
$$f_{12} = k\cdot\left(x_2\right)^{\frac{3}{2}}, \quad x_2 = \max\left(R - \left(z_2 - z_1\right)/2, 0\right), \tag{2.6}$$

where R is the common ball radius and k is the elastic ("spring") constant.

The corresponding Hamiltonian of the system is therefore

$$H = \sum_{i=1,2}\left(\frac{1}{2}m_i v_i^2 + m_i g z_i + E_{ci},\right), \tag{2.7}$$

where the elastic collisional energy is

$$E_{ci} = \frac{2}{5}k\cdot\left(x_i\right)^{\frac{5}{2}}, \quad i = 1,2\,. \tag{2.8}$$

2.2. Modified Verlet method involving second-order mid-point rule

The usual Verlet method renders Eqs. (2.1) and (2.2) for each ball as

$$z^{n+1} = z^n + \Delta t\cdot v^n + \frac{1}{2}(\Delta t)^2\cdot f^n\,, \tag{2.9}$$
$$f^{n+1} = f\left(z^{n+1}\right), \tag{2.10}$$
$$v^{n+1} = v^n + \Delta t\cdot\frac{f^{n+1}+f^n}{2}, \tag{2.11}$$

where Δt is the time-step width, the superscript denotes the time step, and the subscript denoting a particular ball has been omitted.

However, on introducing truncated Taylor series into the model, Eqs. (2.1) and (2.2) become

$$\frac{dz}{dt} + \frac{\Delta t}{2}\frac{d^2z}{dt^2} + \frac{(\Delta t)^2}{6}\frac{d^3z}{dt^3} = v + \frac{\Delta t}{2}f\,, \tag{2.12}$$
$$\frac{dv}{dt} + \frac{\Delta t}{2}\frac{d^2v}{dt^2} + \frac{(\Delta t)^2}{6}\frac{d^3v}{dt^3} = f + \frac{\Delta t}{2}f'v + \frac{(\Delta t)^2}{4}\left(f''v^2 + f'f\right), \tag{2.13}$$

where

$$f'v=\sum_{j=1}^{2}\frac{\partial f\left(z_1,z_2\right)}{\partial z_j}v_j,\quad f''v^2=\sum_{i,j=1}^{2}\frac{\partial^2 f\left(z_1,z_2\right)}{\partial z_i\partial z_j}v_iv_j,\quad f'f=\sum_{j=1}^{2}\frac{\partial f\left(z_1,z_2\right)}{\partial z_j}f_j.$$

The first-order perturbed terms of the time derivative may be eliminated using the equations themselves and the second-order perturbed terms of the time derivative repeatedly, yielding the system of differential equations

$$\frac{dz}{dt}=v-\frac{(\Delta t)^2}{6}\left(f'v\right)\ , \tag{2.14}$$

$$\frac{dv}{dt}=f+(\Delta t)^2\left(\frac{1}{12}f''v^2+\frac{1}{12}f'f\right), \tag{2.15}$$

which produces the modified Verlet method involving the second-order mid-point rule as follows.

On eliminating second-order perturbed terms, and replacing the trapezoidal rule used in the velocity equation in the Verlet method with another formula, one obtains

$$z^{n+1/2}=z^n+\frac{\Delta t}{2}\cdot v^n+\alpha(\Delta t)^2f\left(z^n\right)\ , \tag{2.16}$$

$$v^{n+1}=v^n+\Delta t\cdot f\left(z^{n+1/2}\right)\ , \tag{2.17}$$

where the improved Euler method corresponds to $\alpha=0$ and the mid-point method when $\alpha=1/4$, where the value of the mid-point is $(z^{n+1}+z^n)/2$. Further, the value at the mid-point is given by the Taylor expansion of $z^{n+1/2}$ up to second order if $\alpha=1/8$, under a method designated here as the second-order mid-point rule. The corresponding approximate velocity equation is

$$\frac{dv}{dt}=f+(\Delta t)^2\left(-\frac{1}{24}f''v^2-\frac{1}{24}f'f\right)\ . \tag{2.18}$$

The detailed of derivation of (2.18) is shown in the Appendix.

The perturbed term is cancelled by the weighted average of the equations of the trapezoidal rule and the second-order mid-point rule, such that

$$v_V^{n+1}=v^n+\Delta t\cdot\frac{f\left(z^n+\Delta t\cdot v^n+(\Delta t)^2f\left(z^n\right)/2\right)+f\left(z^n\right)}{2}, \tag{2.19}$$

$$v_T^{n+1}=v^n+\Delta t\cdot f\left(z^n+\frac{\Delta t}{2}v^n+\frac{(\Delta t)^2}{8}f\left(z^n\right)\right)\ , \tag{2.20}$$

$$v^{n+1}=\frac{v_V^{n+1}+2v_T^{n+1}}{3}. \tag{2.21}$$

The appropriate modified equation of position for the new method, derived from (2.14) and the weight of (2.21), is

$$\frac{dz}{dt} = v + \frac{(\Delta t)^2}{12}\left(f'v\right) \tag{2.22}$$

such that

$$z^{n+1} = z^n + \Delta t \cdot v^n + \frac{(\Delta t)^2}{4}\left(f\left(z^n + \Delta t \cdot v^n + \frac{(\Delta t)^2}{2} f\left(z^n\right)\right) + f\left(z^n\right)\right). \tag{2.23}$$

Averaging the corresponding equation in the Verlet method and this equation, using the same weight as for the velocity equation, yields

$$\begin{aligned} z^{n+1} &= z^n + \Delta t \cdot v^n + \frac{(\Delta t)^2}{3} f\left(z^n\right) + \frac{(\Delta t)^2}{6} f\left(z^n + \Delta t \cdot v^n + \frac{(\Delta t)^2}{2} f\left(z^n\right)\right) \\ &= z^n + \Delta t \cdot v^n + \frac{(\Delta t)^2}{2} f\left(z^n\right) + \frac{(\Delta t)^2}{6}\left(f\left(z^n + \Delta t \cdot v^n + \frac{(\Delta t)^2}{2} f\left(z^n\right)\right) - f\left(z^n\right)\right). \end{aligned} \tag{2.24}$$

Equations of (2.19)–(2.21) and (2.24) constitute the modified Verlet method involving the second-order mid-point rule, where one may note that the model equations of the previous subsection are approximated by difference equations to third-order accuracy.

2.3. An harmonic oscillator

The stability of the modified Verlet method involving the second-order mid-point rule can be demonstrated by application to an harmonic oscillator, which can be viewed as a linearised model of one ball striking the floor, where the initial height of the centre of the ball is its radius and the elastic force of restitution is Hooke's law. Thus the ball is deformed by gravity such that the position of the centre of the ball is lowered and then rebounds to its initial height, and subsequently undergoes a continuous harmonic oscillation. Assuming the angular velocity of the harmonic oscillation to be 1.0 radian $\sec^{-1}$ say, the modified Verlet method involving the second-order mid-point rule in this case is

$$\begin{pmatrix} z^{n+1} \\ v^{n+1} \end{pmatrix} = \begin{pmatrix} 1 - \frac{(\Delta t)^2}{2} + \frac{(\Delta t)^4}{12} & \Delta t - \frac{(\Delta t)^3}{6} \\ -\Delta t + \frac{(\Delta t)^3}{6} & 1 - \frac{(\Delta t)^2}{2} \end{pmatrix} \begin{pmatrix} z^n \\ v^n \end{pmatrix}. \tag{2.25}$$

The eigenvalues of the coefficient matrix are complex conjugates, with absolute value $\sqrt{1-(\Delta t)^6/72}$. Thus the computed amplitude of the oscillation is less than the exact amplitude, and accurate to sixth order in the time-step width.

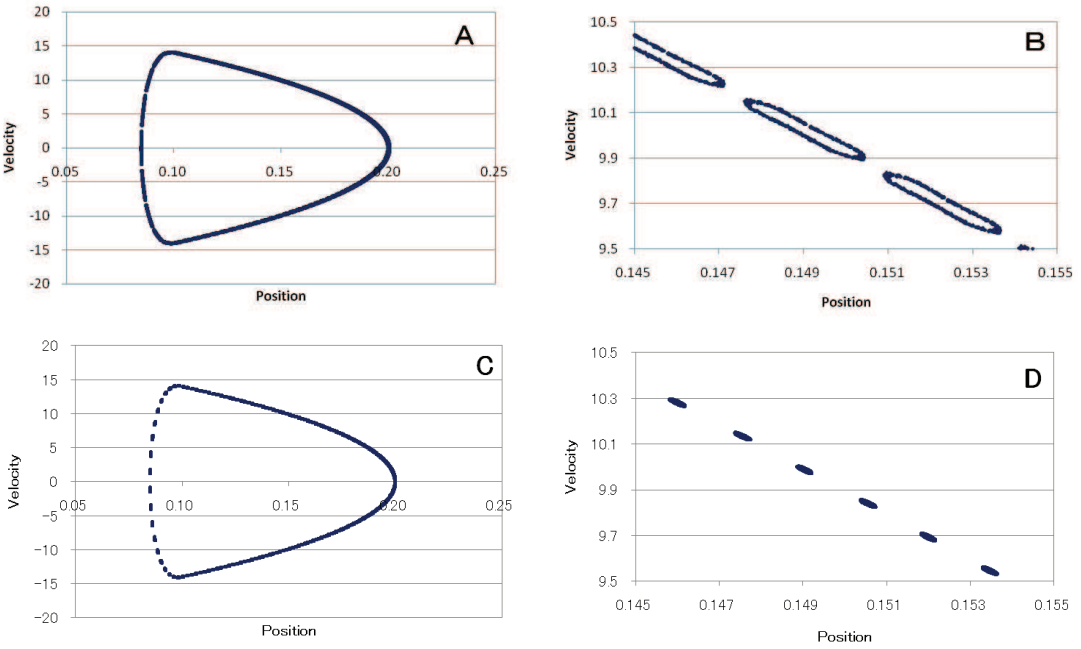

Figure 1: Phase portrait of a bouncing ball: (A),(B) Verlet method; (C),(D) modified Verlet method involving second-order mid-point rule.

2.4. Single bouncing ball

A single bouncing ball also demonstrates the relative advantage of the modified Verlet method involving the second-order mid-point rule. Let us consider a ball of radius 0.1 cm falling until it strikes the rigid floor, where it becomes deformed but is again undeformed on returning to its initial height, and this repeats endlessly. The gravitational acceleration is 980 gm/sec^2, the assumed elastic ("spring") constant of the Hertz theory is 10^7 gm/(cm$^{1/2}\cdot$ sec^2), the assumed initial height of the centre of the ball is 0.2 cm, and the time-step width adopted is 0.0003 sec. The resulting phase portrait obtained from the usual Verlet method is shown in Fig. 1A, and Fig. 1B is an enlargement of a part of 1A. The phase portrait obtained from the modified Verlet method involving the second-order mid-point rule is presented in Fig. 1C, and Fig. 1D is an enlargement of Fig. 1C. Since the total energy is constant, the phase portrait should be a single closed line, but there is a large fluctuation of the phase portrait in Fig. 1B.

It is instructive to note that the approximate Hamiltonian under the Verlet method is

$$H_V = H_{exact} + (\Delta t)^2 \left(-\frac{1}{12} f' v^2 - \frac{1}{24} f^2 \right) , \tag{2.26}$$

where H_{exact} is the exact Hamiltonian. On the other hand, the approximate Hamiltonian

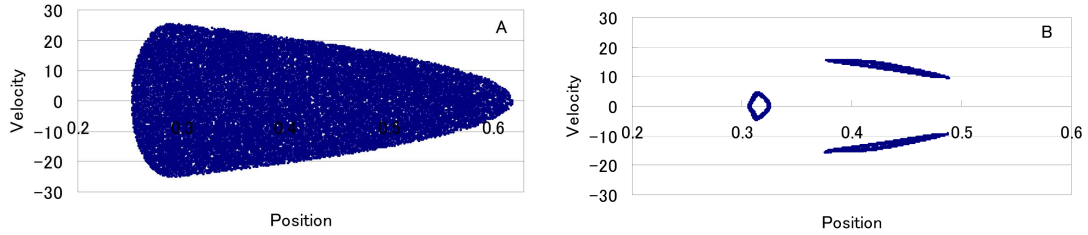

Figure 2: First return map of the upper ball from the modified Verlet method involving second-order mid-point rule. The lower ball mass is (A) 1.2, (B) 0.8, and the upper ball mass is 1.0. The first return map shows the upper ball's position and velocity when the lower ball is in its lowest position after colliding with the floor.

under the second-order mid-point rule in the modified Verlet method is

$$H_T = H_{exact} + (\Delta t)^2 \left(\frac{1}{24} f' v^2 + \frac{1}{48} f^2 \right) , \tag{2.27}$$

where the second-order terms of the Hamiltonian are cancelled out. The suppression of the fluctuation in Fig. 1D is evidence for the improved accuracy under the modified Verlet method involving the second-order mid-point rule.

2.5. Two falling balls

Let us now proceed to simulate the one-dimensional motion of the two balls of finite size falling under gravity. After colliding with the floor, the lower ball either rebounds upward and subsequently collides with the falling upper ball or it eventually falls down again if the two balls do not collide. When the two balls do collide, the momentum exchange returns the lower ball toward the floor and sends the upper ball upward, before that ball falls again. The rhythm of the interaction is obviously complex, and depends upon the relative masses of the two balls.

In the simulation, it is assumed that the initial positions of the ball centres are 0.2 cm and 0.5 cm from the floor, respectively. The period of computation considered is 1000 sec, the time step is 10^{-4} sec, and the other parameters adopted are the same as in the calculation for the single bouncing ball described in the previous subsection. The first return map proposed by Whelan et al. [15] represents the position and velocity of the upper ball when the lower ball is at its lowest position after colliding with the floor. The results from the modified Verlet method involving the seconf-order mid-point rule are presented in Fig. 2, where the mass of the upper ball is 1.0 gm, and that of the lower ball is either 1.2 gm (in Fig. 2A) or 0.8 gm (in Fig. 2B).

The behaviour is chaotic when the upper ball is lighter than the lower ball, but there is quasi-periodicity when the upper ball is heavier, in agreement with theory [15, 16].

Results obtained using other methods are shown in Fig. 3, for the case where the mass of the upper ball is 1.0 gm and that of the lower ball is 0.8 gm. Figs. 3A and 3B present results from the explicit second order symplectic Verlet method, for the time-step

width 10^{-4} sec in Fig. 3A and 10^{-5} sec in Fig. 3B, respectively. It is notable that Fig. 3A is qualitatively different from Fig. 2, which was obtained using the modified Verlet method involving the second-order mid-point rule. Figs. 3C and 3D show the results obtained using a Runge–Kutta method with the time-step width 10^{-4} sec. Fig. 3C shows results from the fourth order 1/6 formula and 3D from the third order Kutta formula that are called RK41 and RK32, respectively [1]. The number of function evaluations per time step is four for the 1/6 formula and three for the Kutta formula, whereas the number of function evaluations per time step in the modified Verlet method involving the second-order mid-point rule is three. Fig. 3D is obviously very different from the others. Fig. 3E presents the result from the symmetric and symplectic implicit mid-point rule with the same time-step width 10^{-4} sec, but it requires evaluation of the right-hand side function of the differential equation at every inner iteration. The convergence criterion value demanded for the inner iteration is 10^{-14}, and approximately six iterations are needed during a collision. With the given time-step width and the number of function evaluations involved, the modified Verlet method involving the second-order mid-point rule is evidently computationally superior.

Fig. 4 presents the intermittency of the difference of velocity between the Verlet method and the second-order mid-point rule, over the time interval 500 sec to 501 sec. During free fall, where the velocity is a linear function of time and correspondingly the position is a square function of time, the results of both second-order methods are the same. However, when the lower ball collides with the floor, or when the upper ball collides with the lower one, the results from the two methods differ. During free fall, the results from the usual Verlet method may be used to correct the results from the second-order mid-point rule when a collision is detected.

3. Balls in the Interface Region of Phase Separation in a Two-Liquid Film

The modified Verlet method involving the second-order mid-point rule is now applied to the problem of colliding balls in the two-liquid film. The two-liquid film is formed in a flat horizontal reservoir, where the ends of the liquid film are in contact with the walls of the reservoir. The top of the film is a free surface, and it is assumed that the phases have separated in the two-liquid film. Furthermore, a shallow water approximation is adopted for the film. Balls are submerged in the liquid film, and are aligned on a line passing transversely across the interface region of phase separation. The balls move horizontally due to the force arising from the chemical potential difference between the balls and the liquid, and tend to fall to the bottom of the potential of the coupled system. When one ball collides with another, it is assumed that they interact elastically as before. The ball movement stirs the liquid in the film through the consequent change in the chemical potential.

3.1. Two-phase shallow water equations

For the two-phase flow in the film, a suitable two-fluid model involves two volume fractions and two velocities for the major and minor phases, and a common pressure [5,6].

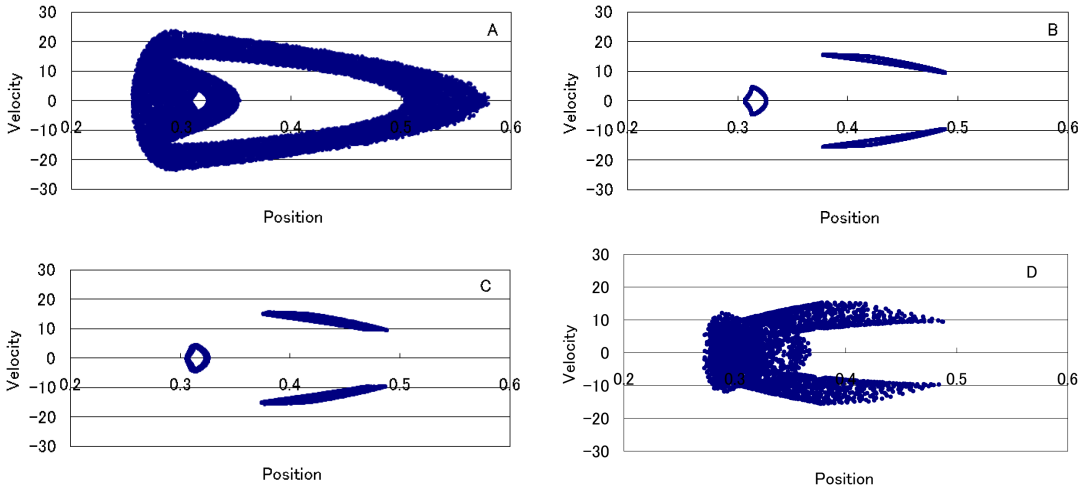

Figure 3: First return map when the masses of the lower and upper balls are 0.8 and 1.0, respectively. The time-step width is 10^{-4} for (A) Verlet method, the time-step width 10^{-5} for the Verlet method in (B), (C) 4th-order Runge–Kutta method and (D) 3rd-order Runge–Kutta method, (E) the implicit mid-point method.

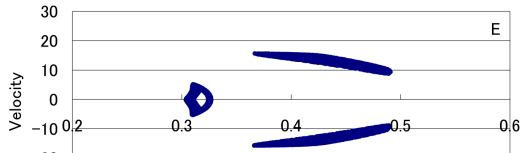

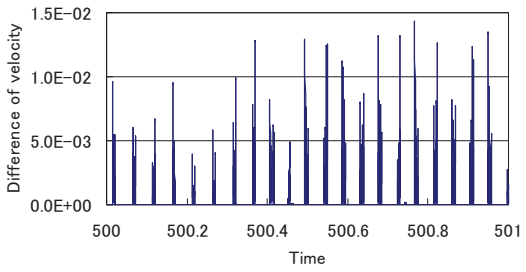

Figure 4: Difference between the upper ball velocities obtained using the usual Verlet method and the second-order mid-point rule.

In a shallow water approximation, the relevant equations are [14]

$$\frac{\partial\left(\alpha_d h\right)}{\partial t}+\frac{\partial\left(\alpha_d h u_d\right)}{\partial x}=0\,, \tag{3.1}$$

$$\frac{\partial\left(\alpha_c h\right)}{\partial t}+\frac{\partial\left(\alpha_c h u_c\right)}{\partial x}=0\,, \tag{3.2}$$

$$\frac{\partial u_d}{\partial t}+u_d\frac{\partial u_d}{\partial x}=-\frac{1}{\rho_d}\frac{\partial\left(\rho_m g h\right)}{\partial x}\,, \tag{3.3}$$

$$\frac{\partial u_c}{\partial t}+u_c\frac{\partial u_c}{\partial x}=-\frac{1}{\rho_c}\frac{\partial\left(\rho_m g h\right)}{\partial x}\,, \tag{3.4}$$

$$\text{where}\qquad \alpha_d+\alpha_c=1\,. \tag{3.5}$$

Here x denotes the horizontal coordinate and t the time, h the surface height, α the volume fractions and u the horizontal velocities where the subscript d denotes the minor phase and c the major phase, g is the gravitational acceleration, and $\rho_m = \alpha_d \rho_d + \alpha_c \rho_c$ is the density of the mixture. The unknowns are the surface height, the two volume fractions, and the two velocities.

The equation for the surface height is derived by adding (3.1), (3.2), and (3.5)

$$\frac{\partial h}{\partial t} + \frac{\partial \left(\alpha_d h u_d + \alpha_c h u_c\right)}{\partial x} = 0. \tag{3.6}$$

The volume fractions are then determined from (3.1) and (3.2), and the equation (3.6) for the surface height.

3.2. Modelling the phenomena in the two-liquid film

The ball motion in the two-liquid film is governed by three interactions – viz. ball–ball interaction, liquid–liquid interaction, and liquid–ball interaction. For the ball–ball interaction, once again elastic collisions are assumed; for the liquid–liquid interaction, the Ginzburg–Landau model for phase separation is adopted; and for the liquid–ball interaction, a phenomenological model proposed in polymer science is used.

The Ginzburg–Landau model defines the Gibbs free energy of the phase separation [2], where the driving forces are given by

$$f_d = -\alpha_d \frac{\partial \mu}{\partial x}, \qquad f_c = \alpha_c \frac{\partial \mu}{\partial x}, \tag{3.7}$$

$$\mu = -a\psi + b\psi^3 - \gamma \frac{\partial^2 \psi}{\partial x^2}, \quad \psi = \alpha_d - \alpha_c. \tag{3.8}$$

Here f represents the driving forces of the phase separation (with subscripts d and c denoting the respective minor and major phases as before), μ is the chemical potential, ψ is the order parameter that distinguishes the phase state by the difference of the volume fractions for the phase separation, and $\{a, b, \gamma\}$ are the constants in the Ginzburg–Landau model that depend on the relevant phenomena.

Adding the driving forces of the phase separation yields the velocity equations in the two-phase shallow water approximation

$$\frac{\partial u_k}{\partial t} + u_k \frac{\partial u_k}{\partial x} = -\frac{1}{\rho_k} \frac{\partial}{\partial x} \left(\rho_m g h \pm \mu\right), \quad k = d, c\,, \tag{3.9}$$

where k is either d or c and the sign of μ is either $+$ for d or $-$ for c.

The phenomenological model adopted for the free energy F_{cpl} of the coupled system is (cf. Peng et al. [9])

$$F_{cpl} = \int dx \left\{ h(x) 4\pi R^2 V\Big(x - r_p\Big) \left(\psi(x) - \psi_s\right)^2 \right\}, \tag{3.10}$$

$$V\Big(x - r_p\Big) = V_0 \exp\left(-\left|x - r_p\right| / r_0\right)\,,$$

where r_p denotes the position of the centre of the ball, ψ_s the order parameter of the surface of the balls, and V_0 and r_0 are constants. When there are two or more more balls in the two-liquid film, their free energies are superposed. The chemical potential of the coupled system is defined by

$$\mu_{cpl} = 8\pi R^2 V \left(x - r_p\right) \left(\psi - \psi_s\right) , \tag{3.11}$$

and added to the chemical potential term of the two-phase shallow water equations.

The velocity equation of a ball of velocity v and mass m in the interface region of phase separation is thus

$$\frac{dv}{dt} = -M \frac{\partial F_{cpl}}{\partial r_p} + f_{collision}/m , \tag{3.12}$$

where M denotes its mobility. When the ith ball collides with the $(i+1)$th ball, the relevant collision term is

$$f_{collision} = k \cdot \left(r_{i,i+1}\right)^{\frac{3}{2}} , \tag{3.13}$$

$$r_{i,i+1} = \max\left(R - \left(r_{p,i+1} - r_{p,i}\right)/2, 0\right) , \tag{3.14}$$

where $r_{p,i}$ is the position of the centre of the i-th ball and the balls are numbered in ascending order from left to right.

3.3. Numerical methods

The modified Verlet method involving the second-order mid-point rule is used in (3.12) to simulate the ball motion in the two-liquid film, using a third-order spline interpolation in the first term on the right-hand side to evaluate the integral representing F_{cpl} given in Eq. (3.10).

For the two-phase shallow-water equations, an invariant finite difference scheme based on the theory of the transformation group and developed by Russian researchers quite accurately resolves the interface region of phase separation [14]. The differential equations of mathematical physics do not alter in form under point transformations (such as the Galilean or similarity transformations), and finite difference schemes can be defined accordingly – i.e. such that the first differential approximation of the finite difference scheme on the discrete points in space and time preserves this property under point transformations [10, 12, 13]. The first differential approximation in the finite difference scheme of [10], where it is also called the modified equation [7], is a partial differential equation obtained by expanding in Taylor series and neglecting higher order terms. Our scheme here is as follows:

$$
\begin{aligned}
&\frac{(\alpha h)_i^{n+1}-(\alpha h)_i^n}{\Delta t}+\frac{(\alpha h u)_{i+1}^n-(\alpha h u)_{i-1}^n}{2\Delta x}\\
=&\frac{\Delta t}{2}\left(u_{i+1/2}^n u_{i+1/2}^n\left((\alpha h)_{i+1}^n-(\alpha h)_i^n\right)-u_{i-1/2}^n u_{i-1/2}^n\left((\alpha h)_i^n-(\alpha h)_{i-1}^n\right)\right)/\Delta x^2\\
&+\Delta t\left(u_{i+1/2}^n(\alpha h)_{i+1/2}^n\left(u_{i+1}^n-u_i^n\right)-u_{i-1/2}^n(\alpha h)_{i-1/2}^n\left(u_i^n-u_{i-1}^n\right)\right)/\Delta x^2\\
&+\frac{\Delta t}{2}\frac{1}{\rho}\left((\alpha h)_{i+1/2}^n\left(\left((\rho_m g h)_{\mathrm{i+1}}^{\mathrm{n}}\pm\mu_{\mathrm{i+1}}^{\mathrm{n}}\right)-\left((\rho_m g h)_{\mathrm{i}}^{\mathrm{n}}\pm\mu_{\mathrm{i}}^{\mathrm{n}}\right)\right)\right.\\
&\left.-(\alpha h)_{i-1/2}^n\left(\left((\rho_m g h)_{\mathrm{i}}^{\mathrm{n}}\pm\mu_{\mathrm{i}}^{\mathrm{n}}\right)-\left((\rho_m g h)_{\mathrm{i-1}}^{\mathrm{n}}\pm\mu_{\mathrm{i-1}}^{\mathrm{n}}\right)\right)\right)/\Delta x^2, \qquad (3.15)
\end{aligned}
$$

$$
\begin{aligned}
&\frac{u_i^{n+1}-u_i^n}{\Delta t}+\frac{u_{i+1}^n+u_{i-1}^n}{2}\frac{u_{i+1}^n-u_{i-1}^n}{2\Delta x}\\
=&-\frac{1}{\rho}\frac{\left((\rho_m g h)_{i+1}^n\pm\mu_{i+1}^n\right)-\left((\rho_m g h)_{i-1}^n\pm\mu_{i-1}^n\right)}{2\Delta x}\\
&+\frac{\Delta t}{2}\left(u_{i+1/2}^n u_{i+1/2}^n\left(u_{i+1}^n-u_i^n\right)-u_{i-1/2}^n u_{i-1/2}^n\left(u_i^n-u_{i-1}^n\right)\right)/\Delta x^2\\
&+\frac{\Delta t}{2}\frac{1}{\rho}(u_{i+1/2}^n\left(\left((\rho_m g h)_{\mathrm{i+1}}^{\mathrm{n}}\pm\mu_{\mathrm{i+1}}^{\mathrm{n}}\right)-\left((\rho_m g h)_{\mathrm{i}}^{\mathrm{n}}\pm\mu_{\mathrm{i}}^{\mathrm{n}}\right)\right)\\
&-u_{i-1/2}^n\left(\left((\rho_m g h)_{\mathrm{i}}^{\mathrm{n}}\pm\mu_{\mathrm{i}}^{\mathrm{n}}\right)-\left((\rho_m g h)_{\mathrm{i-1}}^{\mathrm{n}}\pm\mu_{\mathrm{i-1}}^{\mathrm{n}}\right)\right))/\Delta x^2\\
&+\frac{\Delta t}{2}\frac{1}{\rho}\left(\left(\left((\rho_m g h)_{\mathrm{i+1}}^{\mathrm{n}}\pm\mu_{\mathrm{i+1}}^{\mathrm{n}}\right)(u_m)_{\mathrm{i+1}}^{\mathrm{n}}\right)\right.\\
&\left.-2\left(\left((\rho_m g h)_{\mathrm{i}}^{\mathrm{n}}\pm\mu_{\mathrm{i}}^{\mathrm{n}}\right)(u_m)_{\mathrm{i}}^{\mathrm{n}}\right)+\left(\left((\rho_m g h)_{\mathrm{i-1}}^{\mathrm{n}}\pm\mu_{\mathrm{i-1}}^{\mathrm{n}}\right)(u_m)_{\mathrm{i-1}}^{\mathrm{n}}\right)\right)/\Delta x^2. \qquad (3.16)
\end{aligned}
$$

Here Δt is the time-step size, Δx is the width of the x-directional mesh, the subscript i denotes the x-directional mesh number, n the time step number, and u_m represents the mass-weighted velocity of the mixture – i.e. such that $\rho_m u_m = \alpha_d \rho_d u_d + \alpha_c \rho_c u_c$. The subscripts d and c have now been omitted, since the finite difference scheme for the major phase is the same as that for the minor phase. The use of truncated Taylor series expansions produces the first differential approximation, where first-order terms in Δt and Δx do not appear. The scheme accuracy is second order in time and second order in space [14].

A non-conservative form for the velocity equation is used, although the conservative form is usually chosen. It is necessary to use the conservative form for the computation of shock waves, but shock waves do not play an important role in the problem discussed here. However, there are some phenomenological terms in the mathematical model adopted above – and experience with nuclear code development has revealed that a non-conservative form may be preferable, as the relevant conservative form conserves non-physical errors arising from phenomenological terms [3].

3.4. Preliminary cases: kink solution and two balls in the potential of a kink solution

Prior to the simulation balls in the two-phase flow, two preliminary uncoupled problems were considered. The first was a steady state kink solution for two-phase flow in the film, and the second was for two balls in the potential of a kink solution.

The Euler–Lagrange equation of the Ginzburg–Landau model has an analytic solution called a kink solution, where a one-dimensional two-phase flow is stationary and attains a ground state in the far field – viz.

$$\psi(x) = \psi_e \tanh\left(x/\sqrt{2\xi}\right), \tag{3.17}$$

where $\psi_e = \sqrt{a/b}$ represents the ground state and $\xi = \sqrt{\gamma/a}$ is the order of the interface region thickness [2]. For the numerical computation of this kink solution, a phenomenological lateral viscosity term was added to the equation of velocity – viz.

$$\nu \frac{\partial^2 u_k}{\partial x^2} \simeq \nu \frac{u_{k,i+1} - 2u_{k.i} + u_{k,i-1}}{\Delta x^2}, \quad k = d, c$$

where ν is the phenomenological viscosity coefficient. The introduction of this viscosity term can ensure that the velocity due to the large force due to the phase separation in the interface region decays, such that the numerical solution is stationary.

A steady state was computed from a perturbed kink solution, for the following parameters. The liquid film length was 50 cm and initial height 1.0 cm, the liquid density 1.0 gm/cm^3 and viscosity 0.01 cm^2/sec for the respective phases, and the gravitational acceleration 980 cm/sec^2. The initial velocity of the flow in the film was zero, and the constants in the Ginzburg–Landau model were 1.0 gm/(cm $\cdot$ sec^2) for a and b, and 1.0 gm $\cdot$ cm/sec^2 for γ. The initial distribution of the order parameter was given by the kink solution of the Ginzburg–Landau model. A perturbation of less than 0.0001 was randomly added to the volume fractions of the kink solution, and the space mesh size was 0.1 cm. The origin of the coordinate system centre was taken to be at the centre of the interface region at the centre of the film, the interface region width approximately 6 cm, and the order parameter to be zero at the origin. The boundary conditions assumed at the end of the film were Neumann zero for the volume fractions of the two phases and the surface height, and Dirichlet zero for the velocities. For the time-step width 0.001 sec, the perturbation decayed slowly in the small fluid motion and the calculation converged to the kink solution. The computed steady state of the liquid film for the x-coordinate between -10 cm and 10 cm is shown in Fig. 5. (When the time-step width was 0.01 sec, the computation diverged.)

The second problem involved two balls placed symmetrically about the centre of the potential of the kink solution. This is similar to the bouncing ball problem except for the included potential if symmetry is maintained, where each ball moves toward the centre of the interface region under the chemical potential, the point at which they collide. (The balls are deformed on impact and then move back to their initial positions, before resuming

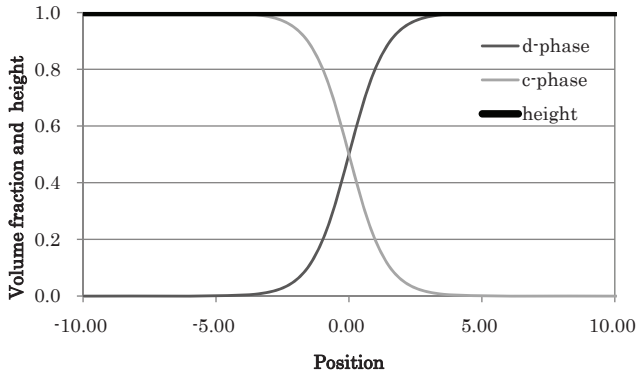

Figure 5: Steady state of the liquid film, from a perturbed kink solution.

their former motion toward the centre.) The radius of each ball was taken to be 0.1 cm, their mass 1.0 gm and the elastic ("spring") constant 10^7 gm/(cm$^{1/2}$sec^2). The assumed initial positions of the balls were ± 0.2 cm, within the interface region of the kink solution. The phase portrait obtained over every 100 steps is shown in Figs. 6A, 6B. The time-step width in Fig. 6A was 0.0001 sec, and 0.0008 sec in Fig. 6B. Since the total energy of the balls is constant, the phase portrait should be a single closed line, but it becomes broadened in Fig. 6B. The maximum position of the ball at the right during two collisions, which we call the peak and should be constant, is shown in Fig. 6C. It is seen that the peak for the time-step width 0.0001 sec does remain approximately constant, with a maximum relative error to the initial position -4.31×10^{-5}. For the time-step widths 0.00055 sec and 0.0008 sec, the peaks are 0.194 cm and 0.173 cm, respectively. Fig. 6D shows the phase portrait of a single ball starting from $x = -0.2$ cm until 500 sec, with the time-step width 0.0008 sec. The decay is negligible in Fig. 6D, meaning that the decay originates from the calculation of collisions. The greater decay of the peak for a larger time-step may be expected qualitatively, on recalling the form for the absolute value of the eigenvalues in Section 2.3.

As foreshadowed, it is the computation of the ball motion that places the main restriction on the time-step in the coupled problem.

3.5. Balls in the interface region of phase separation in a liquid film

Let us now turn to the simulation of four balls in the interface region of a phase-separated film. The liquid films are presumed uniform from the bottom to the surface in the shallow water approximation, so the force applied to the balls through the chemical potential is horizontal. There is no vertical gravitational force on the balls in the liquid film if the densities of the liquid and the balls are equal, so the balls only move horizontally. The effect by which the balls exclude the fluid is ignored.

When the order parameter of the surface of the balls is equal to that of the centre of the interface region and the initial positions of the balls are symmetric about the centre,

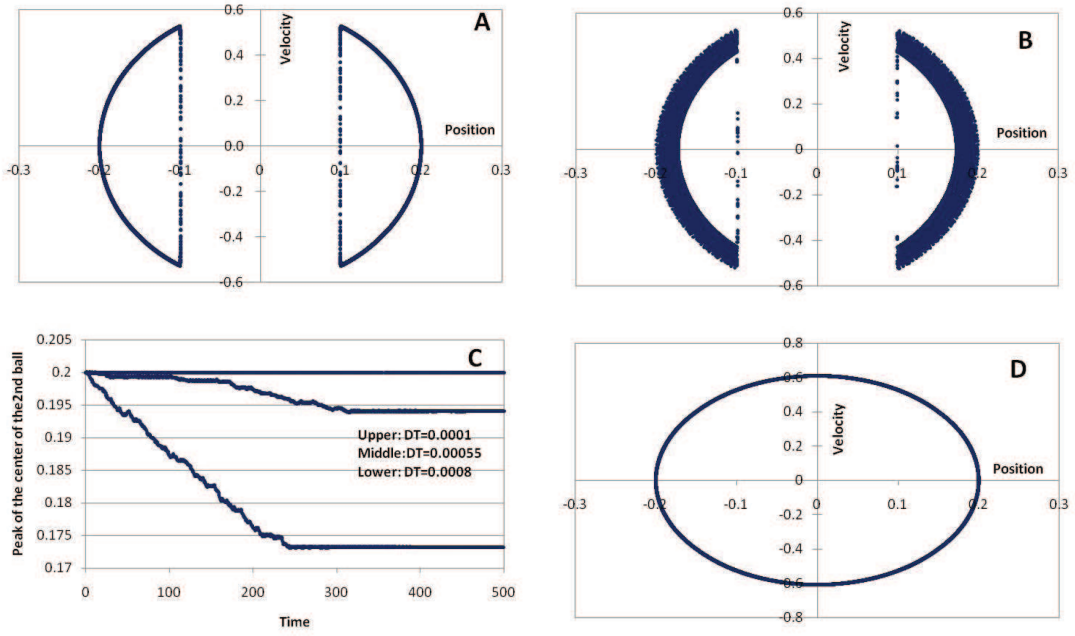

Figure 6: Phase portrait of two balls in the potential of the kink solution, using the modified Verlet method involving second-order mid-point rule: (A) with time-step width 0.0001; (B) with time-step width 0.0008; (C) at the peak position of the right ball; and (D) the phase portrait of a single ball for time-step width of 0.0008.

the balls fall symmetrically toward the centre under the chemical potential. The motion on either side of the centre resembles the case of the two balls falling under constant gravity discussed in Section 2.5, if the symmetry is maintained. Each inner falling ball now collides elastically with the other at the centre, and then moves outward before colliding with the respective outer falling ball or falls again if that collision does not occur. When an inner and outer ball collide, their momentum exchange sends the inner ball back toward the centre and the outer ball moves away, until it again falls toward the centre under the chemical potential. Furthermore, the liquid in the film is stirred by the motion of the balls due to the chemical potential. A sketch of the geometry of the balls in the interface region is illustrated in Fig. 7.

The computational methods for both the ball motion and the two-phase flow are explicit, where values at the $n+1-th$ time step are computed from values of the $n-th$ step and the computation is combined at the $n-th$ step. The assumed properties of the balls and the specification of the two-phase flow in the liquid film was the same as in the previous uncoupled case. The elastic ("spring") constant of the Hertz theory assumed was $10^7\,\mathrm{gm}/(\mathrm{cm}^{1/2}\cdot\mathrm{sec}^2)$, the initial positions of the ball centres were -0.5, -0.2, 0.2 and 0.5 cm, the constant V_0 in the model of the coupled free energy $0.01\,\mathrm{gm}/(\mathrm{cm}^3\cdot\mathrm{sec}^2)$, the constant R_0 0.5 cm, and the ball mobility 10^5 gm^{-1}. The order parameter of the ball surface was zero, the computation time 50 sec, and the time-step width 1.0^{-5} sec (a smaller time-step for the coupled system than for uncoupled cases). Fig. 8A shows the first return

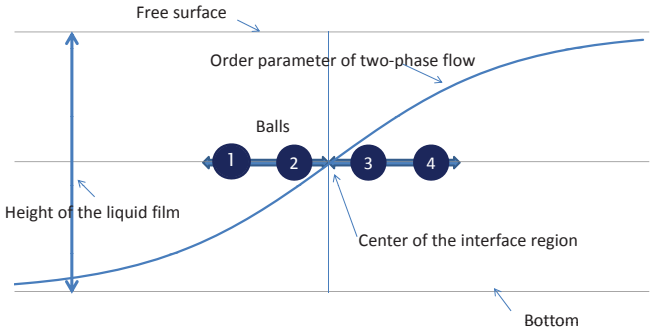

Figure 7: Sketch of the geometry of the balls in the interface region.

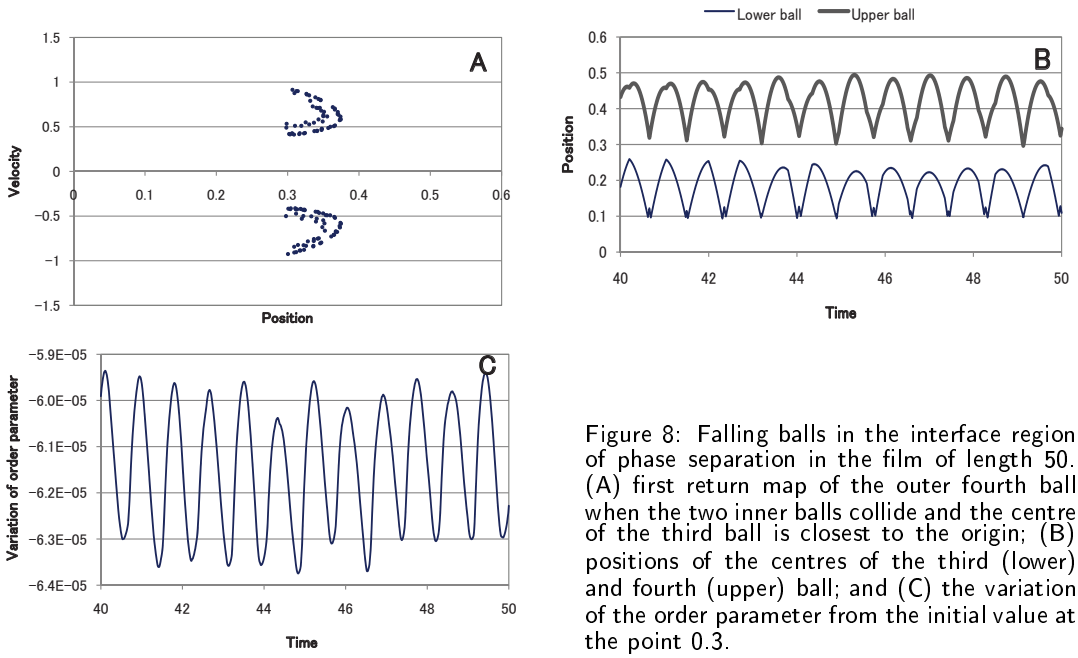

Figure 8: Falling balls in the interface region of phase separation in the film of length 50. (A) first return map of the outer fourth ball when the two inner balls collide and the centre of the third ball is closest to the origin; (B) positions of the centres of the third (lower) and fourth (upper) ball; and (C) the variation of the order parameter from the initial value at the point 0.3.

map of the outer fourth ball when the two inner balls collide and the centre of the third ball is closest to the origin. Fig. 8B portrays the positions of the centres of the third and fourth balls in the right half of the film during the time interval $40-50$ sec, and of course the movement of the first and second ball in the left half is symmetric. Fig. 8C presents the variation of the order parameter from the initial value $x = 0.3$ cm during the time interval $40-50$ sec. The numerical method evidently resolved the small variation of the order parameter caused by the ball motion.

The first return map depends sensitively on the chemical potential and the dimension of the film. For example, if the length of the film is 50.1 cm rather than 50 cm, a quasi-periodic first return map is obtained, as shown in Fig. 9A. Fig. 9B is an enlargement of the upper right part of Fig. 9A. The other parts of Fig. 9A are also elliptic, but no elliptic

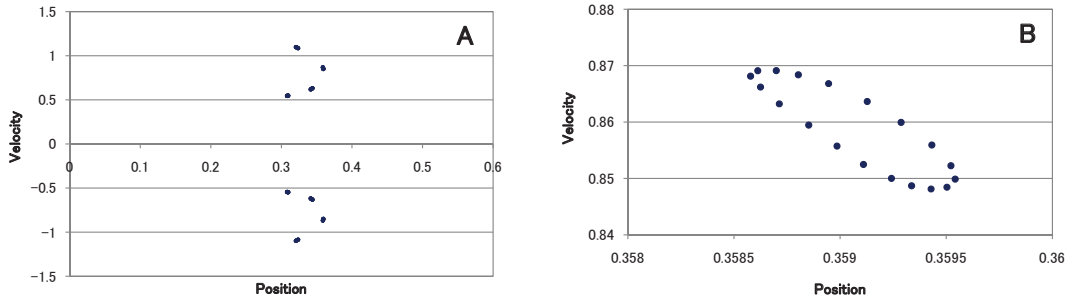

Figure 9: (A) First return map when the length of the film is 50.1; and (B) enlargement of the upper right part of (A).

figures appear in Fig. 8A. A survey of the first return map remains an issue for further study. And the high sensibility on the parameters of the phenomena suggests the possibility and difficulty to control balls for technological purposes.

4. Conclusion

The modified Verlet method involving the second-order mid-point rule is more efficient in the simulation of falling balls than numerical integrators previously used. In particular, the motion of balls under the chemical potential within the interface region of phase separation in a two-liquid film was accurately and efficiently simulated by the modified Verlet method involving the second-order mid-point rule, when combined with an invariant finite difference scheme for the two-phase shallow water equations. However, a more careful consideration of the first return map remains an issue for further study.

A. Appendix

The derivation of equation (2.18) from (2.16) and (2.17) in Section 2.2 is an elimination process involving time differential. The velocity equation using the second-order mid-point rule is

$$\frac{v^{n+1}-v^n}{\Delta t} = f\left(z^n + \frac{\Delta t}{2}\cdot v^n + \alpha(\Delta t)^2 f\left(z^n\right)\right). \tag{A.1}$$

Ignoring higher order terms, the Taylor expansion of (A.1) becomes

$$\frac{dv}{dt} + \frac{\Delta t}{2}\frac{d^2v}{dt^2} + \frac{\Delta t^2}{6}\frac{d^3v}{dt^3} = f + \frac{\Delta t}{2}f'v + \frac{\Delta t^2}{8}f''v^2 + \alpha(\Delta t)^2 f'f, \tag{A.2}$$

where the summations are represented as in Section 2.2.

The second-order and third-order time derivatives on the left-hand side of (A.2) are eliminated by invoking differentiated forms of the equation, to yield

$$\frac{dv}{dt} + \frac{\Delta t}{2}\frac{df}{dt} + \frac{\Delta t^2}{6}\left(f'f + f''v^2\right) = f + \frac{\Delta t}{2}f'v + \frac{\Delta t^2}{8}f''v^2 + \alpha(\Delta t)^2 f'f. \tag{A.3}$$

Similarly, equation (2.16) becomes

$$\frac{dz}{dt}+\frac{\Delta t}{4}\frac{dv}{dt}+\frac{\alpha}{2}(\Delta t)^2\frac{df}{dt}=v+2\alpha\Delta t\cdot f+\frac{1}{48}(\Delta t)^2\frac{d^2v}{dt^2}. \tag{A.4}$$

Substituting (A.3) into (A.4) and ignoring higher order terms, (A.4) becomes

$$\frac{dz}{dt}=v+\Delta t\left(2\alpha-\frac{1}{4}\right)f+(\Delta t)^2\left(\frac{1}{48}-\frac{\alpha}{2}\right)f'v. \tag{A.5}$$

Applying (A.5) to the calculation of the second term in the left-hand side of (A.3) and ignoring the higher order terms, the result is

$$\frac{dv}{dt}=f-(\Delta t)^2\left(\alpha-\frac{1}{8}\right)f+(\Delta t)^2\left(\frac{1}{8}-\frac{1}{6}\right)f''v^2+(\Delta t)^2\left(\alpha-\frac{1}{6}\right)f'f. \tag{A.6}$$

If α is equal to $1/8$, (A.6) becomes

$$\frac{dv}{dt}=f+(\Delta t)^2\left(-\frac{1}{24}f''v^2-\frac{1}{24}f'f\right). \tag{A.7}$$

References

[1] Butcher, J.C. (2003). *Numerical Methods of Ordinary Differential Equations*, Wiley.

[2] Chaikin, P.M., and Lubensky, T.C. (1995). *Principles of Condensed Matter Physics*, Cambridge University Press.

[3] Daly, B.J., and Torrey, M.D. (1984). *SOLA-PTS: a transient, three-dimensional algorithm for fluid-thermal mixing and wall heat transfer in complex geometries* **NUREG/CR-3822; LA-10132-MS**, Technical Report of Los Alamos National Laboratory.

[4] Galperin, G. (1978). Elastic collisions of particles on a line, *Russian Math. Surveys* **33**, 119-200.

[5] Gidaspow, D. (1994). *Multiphase Flow and Fluidization*, Academic Press.

[6] Ishii, M. (1975). *Thermo-fluid dynamics theory of two-phase flow*, Eyrolles.

[7] LeVeque, R.J. (2002). *Finite volume method for hyperbolic problems*, Cambridge University Press.

[8] Lin, Y., Skaff, H., Emrick, T., Dinsmore, A.D., and Russell, T. (2003). Nanoparticle assembly and transport at liquid–liquid interfaces. *Science* **299**, 226–229.

[9] Peng, G., Qiu, F., Ginzburg, V.V., Jasnow, D., and Balazs, A.C. (2000). Forming supramolecular networks from nanoscale rods in binary, phase-separating mixtures. *Science* **288**, 1802–1804.

[10] Shokin, Y.I. (1983). *The Method of Differential Approximation*, Springer-Verlag.

[11] Timoshenko, S.P., and Goodier, J.N. (1970). *Theory of Elasticity*, McGraw Hill.

[12] Yanenko, N.N., and Shokin, Y.L. (1971). On the group classification of the difference schemes for systems of equations of gas dynamics. In *Lecture Notes in Physics* **8** (Holt, M. Ed.), 3-17, Springer.

[13] Yanenko, N.N., and Shokin, Y.L. (1973). Schemes numerique invariants de groupe pour les equations de la dynamique de gas. In *Lecture Notes in Physics* **18**, Cabannes, H., and Temam, R. Eds., 174–186, Springer.

[14] Yasuda, H. (2009). Two-phase shallow water equations and phase separation in thin immiscible liquid films. *Journal of Scientific Computing*, in press. (On-line vr. DOI: 10.1007/s10915-009-9280-6)
[15] Whelan, N.D., Goodings, D.A., and Cannizo, J.K. (1990). Two balls in one dimension with gravity. *Phys. Rev.* **A42**, 742–754.
[16] Wojtkowski, M. (1990). A system of one-dimensional balls with gravity. *Commun. Math. Phys.* **126**, 507-533.
[17] Wojtkowski, M. (1990). The system of one-dimensional balls in an external field. *Commun. Math. Phys.* **127**, 425–432.
[18] Wyrwa, D., Beyer, N., and Schmid, G. (2002). One-dimensional arrangements of metal nanoclusters. *Nano Letters* **2**, 419–321.